Simple method for simultaneous long-term stabilization of relative timing and carrier-envelope phase in waveform synthesis

Pei Huang, Shaobo Fang, Yitan Gao, Kun Zhao, Xun Hou, and Zhiyi Wei

View Online   Export Citation   CrossMark

Applied Physics Letters

Mid-IR and THz frequency combs special collection

Read Now!

Simple method for simultaneous long-term stabilization of relative timing and carrier-envelope phase in waveform synthesis

Pei Huang,[1,2,3,a)] Shaobo Fang,[2,3,a),b)] Yitan Gao,[2,3] Kun Zhao,[2,3] Xun Hou,[1,3] and Zhiyi Wei[2,3]

AFFILIATIONS

[1]State Key Laboratory of Transient Optics and Photonics, Xi'an Institute of Optics and Precision Mechanics of CAS, Xi'an 710119, China
[2]Beijing National Laboratory for Condensed Matter Physics, Institute of Physics, Chinese Academy of Sciences, Beijing 100190, China
[3]University of Chinese Academy of Sciences, Beijing 100049, China

[a)]Contributions: P. Huang and S. Fang contributed equally to this work.
[b)]Author to whom correspondence should be addressed: shaobo.fang@iphy.ac.cn

ABSTRACT

We present an *f*-to-*2f* interferometry method to simultaneously measure and control the relative timing (RT) and carrier-envelope phase (CEP) of an arbitrarily tailored optical-field waveform. Long-term stabilization of the phase-locking system results in a CEP stability of 280 mrad and a RT stability of 110 attosecond over 8 h at a repetition rate of 1 kHz. The synthesized optical field characterized by a transient-grating frequency-resolved optical gating delivers 3.8-fs near single-cycle waveforms. This technique constitutes a versatile tool for coherent pulse synthesis, which can be applied in experiments using a dual-color light field for high-harmonic generation and attosecond timing precision pump-probe spectroscopy.

Published under license by AIP Publishing. https://doi.org/10.1063/1.5083239

The generation of complicated and arbitrarily tailored optical waveforms has attracted enormous attention from the ultrafast laser science community.[1,2] It opens new prospects for the studies of extreme light-matter interactions.[3–5] By coherently synthesizing multiple ultrabroadband spectra, researchers have demonstrated optical field transients to control electron dynamics within a subfemtosecond time window.[6,7] It is well known that producing extremely short waveforms with a transform-limited (TL) pulse width requires accurate dispersion control of the entire bandwidth.[8] Optimization of the synthesized waveforms demands complete spatiotemporal overlap of few-optical-cycle light pulses with different spectra. In parallel synthesis schemes, one of the key enabling technologies for coherent optical waveform synthesizers is the full control of the complete phase (CP) between multiple few-cycle subpulses. The major factors affecting the complete phase are relative timing (RT) and carrier-envelope phases (CEPs) of each subpulse that will be synthesized (CEPs).

Over the past few years, the individual characterization of the RT or CEP has become technically feasible.[9–13] In two-color driving high harmonic generation,[10] the RT between the two pulses should be strictly controlled. In this scheme, a continuous wave (CW) laser is introduced as a reference. A feedback loop based on a balanced optical

cross-correlator (BOC) can lock the RT to less than 30 attoseconds without any CEP-locking.[14] Active or passive stabilization of the non-averaged CEP has been optimized to be better than sub-100-mrad root mean square (RMS) by combining a nonlinear *f*-to-*2f* interferometer and an acousto-optic programmable dispersive filter without any RT locking.[15] For many applications, one would like to have a precise and real-time complete phase measurement with one interferometry.

In this letter, we demonstrate a scheme to stabilize the complete phase for a waveform synthesizer, in which the RT and CEP have been assessed simultaneously using a normal collinear *f*-to-*2f* interferometer. The following proof-of-principle experiments were carried out using an octave-spanning white-light supercontinuum (WLSC: 450–980 nm), which was spectrally divided into two beams, compressed by chirped mirror pairs, and finely tuned by wedge pairs individually. The stability of the complete phase was actively controlled to be 110-as RMS of the RT and 280-mrad RMS of the CEP, resulting in a sub-4-fs optical waveform synthesizer.

In our experimental setup (Fig. 1), the output of a CEP-stable Ti:sapphire amplifier (30 fs, ~1 mJ, 1 kHz) was spectrally broadened in a 1-m neon-filled hollow core fiber with an inner diameter of 250 μm. The transmission through the pressure-gradient hollow fiber
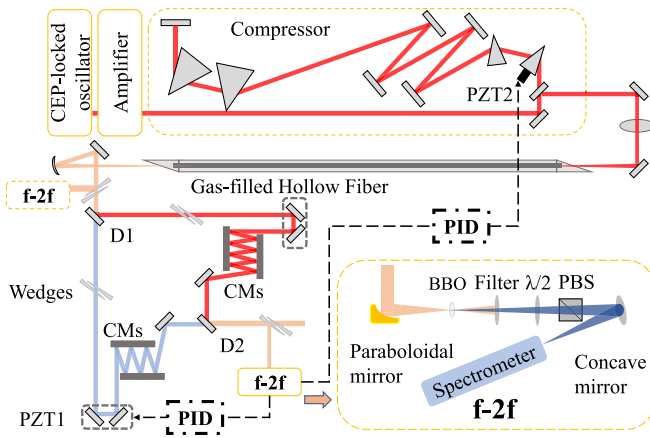
FIG. 1. The experimental setup. PZT: piezotransducer, D (1, 2): dichroic mirrors, PID: proportion-integration-derivative controller, PBS: polarization beam splitter, and $\lambda/2$: half wave plate.

(the input end is close to vacuum and the output end is about 220 kPa) results in a half-millijoule WLSC (450–980 nm), supporting a 3.0 fs TL pulse (Fig. 2). The WLSC was spectrally divided into two beams by a beam splitter (Dichroic mirror: D1), and each beam was individually compressed by a set of the custom-designed double-chirped mirrors and wedge pairs. The short and long wavelength pulses were measured to be 6.4 fs and 7.6 fs, respectively. A two-color interferometer (Fig. 1) was employed to recombine the two pulses to produce waveforms with an ~400 μJ energy and 3.8-fs pulse duration (TL pulse: ~3 fs), which were then focused into a type-I beta-barium borate (BBO) crystal for converting the pulses (~960 nm) from the longer-wavelength part to 2*f* pulses (~480 nm). As a result, the polarization of 2*f* pulses changes, which was perpendicular to that of the *f* pulse
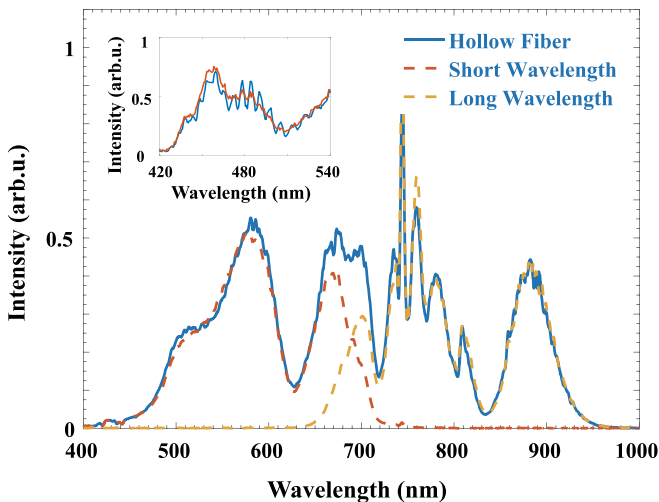
FIG. 2. Optical spectrum of the synthesized pulses. Hollow fiber output spectrum (blue solid curve) and the spectra after the dichroic mirror D1 (red and yellow dashed curves for short and long wavelength channels, respectively). Inset: the interference fringes appear (blue curve) and disappear (red curve) when the RT is close to zero or very far away.

(~480 nm) from the shorter-wavelength part. Both the *f* and 2*f* pulses were sent into a high-resolution spectrometer (Ocean USB 2000+, acquisition time is 3 ms) after propagating through a half-wave plate and a Glan prism for observing interference fringes (Fig. 2 inset).

In order to extract the RT and CEP signals simultaneously from the inverse Fourier transform of the spectral interference for feedback control, the electric fields of the *f* and 2*f* pulses are expressed as

$$E_F(\omega) = \sqrt{I_F(\omega)}e^{i[\varphi_F(\omega)+\varphi_{CE1}]}, \qquad (1)$$

$$E_{SH}(\omega) = \sqrt{I_{SH}(\omega)}e^{i[\varphi_{SH}(\omega)+2\varphi_{CE2}+\omega\Delta t]}, \qquad (2)$$

where $I_F(\omega)$ and $I_{SH}(\omega)$ are the intensities of the fundamental pulse from the white-light supercontinuum directly and the second harmonic of the longer-wavelength part of the fundamental pulse, respectively.[16] Here, $\varphi_F(\omega)$, φ_{CE1} and $\varphi_{SH}(\omega)$, φ_{CE2} are their spectral phases and CEPs, respectively. Since the *f* and 2*f* pulses are simultaneously produced via the same WLSC generation driven by the same input laser pulses, φ_{CE1} is linked to φ_{CE2}. In this case, since the two pulses came from the same source and there are no nonlinear effects in the interferometer to disturb their respective phases, we have $\varphi_{CE2} = \varphi_{CE1} + \Delta\varphi_{CE}$, where $\Delta\varphi_{CE}$ is more or less a constant value. Δt is the RT by which the *f* pulse leads the 2*f* pulse due to the dispersions from their individual optical paths and transmitting components in the *f-2f* device. In the rest of this letter, we define $\varphi_{CE1} = \varphi_{CE}$, $\varphi_{CE2} = \varphi_{CE} + \Delta\varphi_{CE}$.

The interference pattern between the *f* and 2*f* pulses can be expressed as

$$\begin{aligned} I(\omega) &\propto \left|E_F(\omega) + E_{SH}(\omega)\right|^2 \\ &= I_F(\omega) + I_{SH}(\omega) + 2\sqrt{I_F(\omega)I_{SH}(\omega)} \\ &\times \cos(\omega\Delta t + \varphi_{SH}(\omega) - \varphi_F(\omega) + \varphi_{CE} + 2\Delta\varphi_{CE}). \end{aligned} \qquad (3)$$

The CEP (φ_{CE}) and RT (Δt) in the interference term can be extracted by the inverse Fourier transform as in the method of Fourier transform spectral interferometry.[17] Ideally, under phase-matching conditions, the *f* and 2*f* pulses have a frequency-independent relative $\pi/2$-phase shift, predicted by Maxwell's equation.[18] The complete phase from the inverse Fourier transform is

$$\Phi = \omega\Delta t + \pi/2 + \varphi_{CE} + 2\Delta\varphi_{CE}. \qquad (4)$$

However, unlike previous *f*-to-2*f* interferometry, the complete phase variation between the two pulses includes three components: the constant phase shift ($\pi/2 + 2\Delta\varphi_{CE}$), the CEP ($\varphi_{CE}$), and RT ($\Delta t$). Δt is the linear correlation coefficient of the angular frequency (ω). From the contribution of the interference term in Eqs. (3) and (4), the RT is abscissa of the first positive delay peak in the absolute value after inverse Fourier transform of the spectral interferometry signal in Fig. 2, while the complete phase is the ordinate of the argument after inverse Fourier transform for characterizing the CEP in previous interferometry works.[17,19] In this approach, we locked the RT in advance during a time when the CEP fluctuation was negligible. Based on this premise, the resultant complete phase served as the error signal for stabilizing the CEP of the waveform synthesizer through our multiple-loop feedback control system.

The key difference of our setup from most previous works with the conventional inline propagation scheme was that both the CEP of individual subpulses and the RT between them contributed to the

complete phase of the combined waveforms. In our experimental scheme, the RT drift caused by the dispersion from the same optical path within the inline *f*-to-2*f* setup was negligible; the RT variation was dominated by the optical path drift in the two-color interferometer, which provided more flexibility for the delay and dispersion management in a waveform synthesizer. However, the RT drift caused by the interferometer had to be considered as important as the CEP (or complete phase) drift. Because we used a CEP-stable oscillator as the frontend in our laser system, observation of the interference fringes in the region of the spectral overlap became experimentally feasible, as shown in the inset of Fig. 2. Our locking system included a multiple-loop feedback control system with a high-resolution spectrometer and two home-built PID modules. The RT was first locked with a piezo-transducer (PZT1) actuated delay stage in the short wavelength channel of the two-color interferometer to compensate the RT jitter. The CEP was simultaneously locked with a separate delay stage (PZT2) in the prism compressor to precisely stabilize the complete phase.

In our algorithm, to eliminate the effect of CEP drift on RT locking, the selected Fourier transform range is adjusted along with spectral interference fringes when extracting RT signals. We always select the maximum intensity value of interference fringes, and therefore, when the abscissa of the maximum intensity value changes, the Fourier transform range should be changed as well. The wavelength is converted into sampling points of spectrometer pixels with the left-most point in each Fourier transform range calibrated to 0. Each sampling point is reassigned to an integer in turn; after Fourier transform and the division by the number of sample points, the number of fringes is obtained. To verify the performance of complete phase active stabilization, we measured the complete phase drift before the two-color interferometer, as shown in Fig. 3. The complete phase drift was 960 mrad RMS (green curve) without any active stabilization and then minimized to 250 mrad RMS (blue curve) with the feedback control loop. Since there was no RT drift before the two-color interferometer, the complete phase was equivalent to the CEP in this measurement. Under the same experimental conditions, we measured a 440-mrad complete phase drift (red curve) after the beam combiner of the two-color interferometer without locking the RT, where the complete phase was contributed by both the CEPs and the RT between the two pulses.

To improve the stability of the complete phase locking system, we characterized and controlled the RT as well. In order to extract the RT signal from the interference fringes, we first calibrated the delay line. The fringes originated from the interference between the pulses
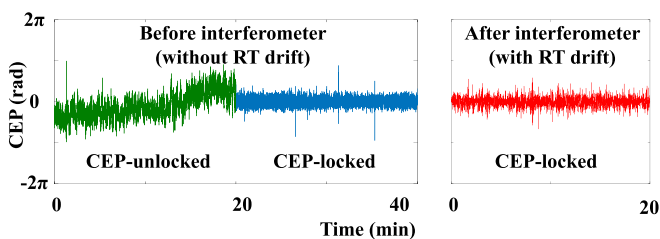
from two different optical paths. The fringe number from the *f*-to-2*f* spectral interference was a function of the time delay between the two pulses. The experimental results (blue curve) and the numerical simulation results (red curve) are shown in Fig. 4(a), in which the two curves showed good agreement. The delay-calibration curve was shown in Fig. 4(a) as the yellow curve. Compared with the straightforward Fourier transform of the spectral interference fringes expressed in optical frequency, we use the "number of fringes" method—which needs to be calibrated—to show the physical phenomena directly related to RT; it also shows that the effect of CEP on RT can be eliminated. Similarly, the straightforward RT calculated by spectral interference fringes is not the real RT because we select only a part of the interference fringes in the spectral domain and convert it into the frequency domain by Fourier transform. Therefore, a calibration is necessary for both the straightforward Fourier transform and the number of fringes method.

The feedback control loop of the RT between the two synthesized subpulses with 120-as precision was a prerequisite for coherent waveform synthesis with 3-fs TL pulse durations (ideally, the RT should be less than a hundredth of the TL pulse duration for a perfect synthesized pulse stream). Specifically, after the interferometer, the synthesized waveforms were stabilized by the CEP- and RT-locking system.

Aiming to investigate the complete phase contribution from the optical waveform synthesizer, we compared the sequences of the
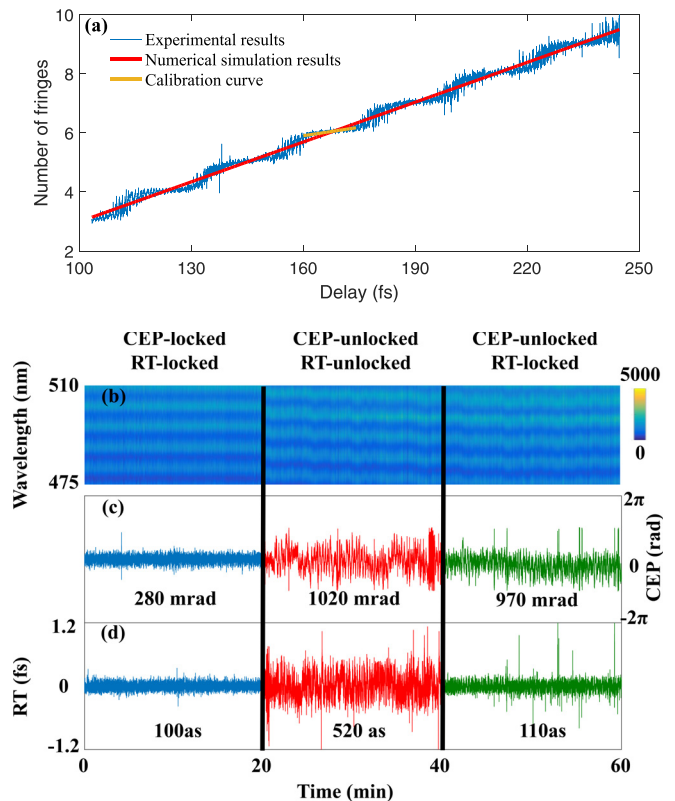
FIG. 4. (a) Number of interference fringes as a function of the time-delay. (b) Sequences of the interferograms in the three cases. (c) Reconstructed CEP fluctuations. (d) Reconstructed RT fluctuations.

FIG. 3. The complete phase (CP) variations when the CEP was unlocked (960 mrad RMS: green) and locked (250 mrad RMS: blue) before the two-color interferometer; the complete phase variation of the CEP-locked (no RT-locking) system after the two-color interferometer (440 mrad RMS: red).

interferograms [Fig. 4(b)] in three typical operation modes as shown in Figs. 4(c) and 4(d):

Case 1 (blue curves): we measured 100-as of the RT and 280-mrad of the CEP variations when both the RT and CEP were locked;
Case 2 (red curves): we measured 520-as of the RT and 1020-mrad of the CEP variations when both the RT and CEP were unlocked;
Case 3 (green curves): we measured 110-as of the RT and 970-mrad of the CEP variations when the only RT was locked.

Obviously, the interference term in formula (3),

$$2\sqrt{I_F(\omega)I_{SH}(\omega)}\cos(\omega\Delta t + \varphi_{CE} + \pi/2 + 2\Delta\varphi_{CE}), \quad (5)$$

showed that the period of the spectral interference fringes was only related to the RT because the term Δt was the linear coefficient of the angular frequency (ω). In this case, the spacing of the spectral interference fringes was fixed when the RT was locked, and the drift of the fringes was only contributed by the CEP.

Intended for many practical applications, a long-term coherent combination of the two-color pulses was achieved over 8 h of recording time. The complete phase and RT drifts were less than 280 mrad RMS and 110 as RMS, respectively (Fig. 5). The residual RT variation was tightly locked within 1/20 optical cycle considering a center wavelength of 700 nm.

The complete phase fluctuation was intrinsically linked to the CEP and RT and therefore can be derived from the locking results of the CEP and RT. Here, we represented the complete phase as

$$\Delta\Phi_T = \omega\Delta t + \varphi_{CE} = (2\pi c/\lambda)\Delta t + \varphi_{CE}, \quad (6)$$

where the center wavelength of the synthesized pulse was 700 nm. Based on the results of the three different cases, the RT fluctuations were calculated to be 270-mrad, 1400-mrad, and 300-mrad for Cases 1–3 (Fig. 4), respectively. As discussed in greater detail in Refs. 4 and 5, the stabilities of the RT and CEP were two key ingredients for generating reproducible arbitrarily tailored electric-field transients. To minimize the RT and CEP variations resulting from environment-induced optical length fluctuations, all optic components were mounted on a temperature-stabilized breadboard with a lead foam for damping the vibrations from the optical-table. The experimental setup was enclosed by a custom-designed sealed housing. Thanks to the careful engineering of the optical paths in this experiment, the RT fluctuation (mainly due to the instabilities in the half-meter long optical paths of the two-color interferometer) was smaller than the CEP fluctuation. For the parallel-scheme optical waveform synthesizers based on the high-energy optical parametric
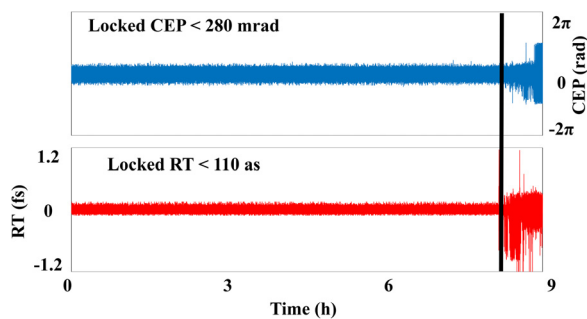
FIG. 5. Long-term stability of the CEP and the RT.
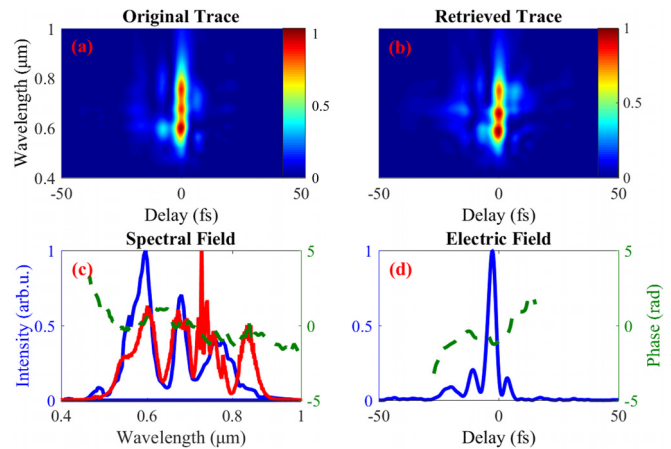
FIG. 6. TG-FROG characterization of the synthesized waveforms. (a) Measured and (b) retrieved TG-FROG traces. (c) Measured spectrum and retrieved spectrum and phase. (d) Retrieved temporal intensity and phase profile.

chirped-pulse amplifiers,[20] the two parent pulses traveled at different optical paths of hundreds of meters long. Compared with stabilization of the environmental conditions, it is more important to minimize the RT fluctuation with an active locking system.

To demonstrate this locking method for broadband synthesis, the complete spectrotemporal characterization was accomplished by a home-built transient-grating frequency-resolved optical gating (TG-FROG).[21] It is noteworthy that the TG-FROG results shown in Fig. 6 were measured at the actual waveform synthesis point. The TG-FROG reconstructions showed that the synthesized pulses were compressed to 3.8 fs FWHM [solid curve in Fig. 6(d)]. In these measurements, we did not compress the full bandwidths to the TL intensity profile (3.0 fs) due to the bandwidth limit of the double-chirped mirror (DCM) pairs (520–980 nm). This proves that our scheme can run well to the few-cycle pulse synthesizer. An independent cross-check of the locked RT, such as a BOC measurement, would establish the locking of the RT in our pulse synthesis definitively, which will be carried out in a separate experiment.

In conclusion, we presented a method for phase characterization of broadband synthesized waveforms.[22] The CEPs and the RT between the two parent pulses were locked simultaneously by a simple f-to-$2f$ device. The proof-of-principle experiments demonstrated that the RT drift was locked by locking the number of spectral interference fringes and the CEP drift was minimized by stabilizing the swing of the spectral interference fringes. The long-term RT stability was achieved to be 110-as RMS, while the residual CEP noise within 8 h amounted to 280-mrad RMS. The accuracy of the f-to-$2f$ stabilization loop was mainly limited by the resolution of the spectrometer and can be as low as sub-100 as. By employing this f-to-$2f$ device, we demonstrated a sub-4-fs, phase-stable, 0.1-TW optical waveform, which is desired for high-energy, multipulse optical waveform synthesis and attosecond transient absorption spectroscopy.

REFERENCES

[1]H. Chan, Z. Hsieh, W. Liang, A. H. Kung, C. K. Lee, C. J. Lai, R. P. Pan, and L. H. Peng, Science **331**, 1165 (2011).

[2]S. W. Huang, G. Cirmi, J. Moses, K. H. Hong, S. Bhardwaj, J. R. Birge, L. J. Chen, E. Li, B. J. Eggleton, G. Cerullo, and F. X. Kärtner, Nat. Photonics **5**, 475 (2011).

[3]F. Krausz and M. Ivanov, Rev. Mod. Phys. **81**, 163 (2009).

[4]O. D. Mucke, S. Fang, G. Cirmi, G. M. Rossi, S. H. Chia, H. Ye, Y. D. Yang, R. Mainz, C. Manzoni, P. Farinello, G. Cerullo, and F. X. Kärtner, IEEE J. Sel. Top. Quantum Electron. **21**, 8700712 (2015).

[5]C. Manzoni, O. D. Mucke, G. Cirmi, S. Fang, J. Moses, S. W. Huang, K. H. Hong, G. Cerullo, and F. X. Kartner, Laser Photonics Rev. **9**, 129 (2015).

[6]A. Wirth, M. Th. Hassan, I. Grguraš, J. Gagnon, A. Moulet, T. T. Luu, S. Pabst, R. Santra, Z. A. Alahmed, A. M. Azzeer, V. S. Yakovlev, V. Pervak, F. Krausz, and E. Goulielmakis, Science **334**, 195 (2011).

[7]M. Th.Hassan, T. T. Luu, A. Moulet, O. Raskazovskaya, P. Zhokhov, M. Garg, N. Karpowicz, A. M. Zheltikov, V. Pervak, F. Krausz, and E. Goulielmakis, Nature **530**, 66 (2016).

[8]S. H. Chia, G. Cirmi, S. Fang, G. M. Rossi, O. D. Mücke, and F. X. Kärtner, Optica **1**, 315 (2014).

[9]T. R. Schibli, J. Kim, O. Kuzucu, J. T. Gopinath, S. N. Tandon, G. S. Petrich, L. A. Kolodziejski, J. G. Fujimoto, E. P. Ippen, and F. X. Kaertner, Opt. Lett. **28**, 947 (2003).

[10]M. Th. Hassan, A. Wirth, I. Grguraš, A. Moulet, T. T. Luu, J. Gagnon, V. Pervak, and E. Goulielmakis, Rev. Sci. Instrum. **83**, 111301 (2012).

[11]L. Xu, Ch. Spielmann, A. Poppe, T. Bravec, and F. Krausz, Opt. Lett. **21**, 2008 (1996).

[12]H. Tian, Y. J. Song, F. Meng, Z. J. Fang, M. L. Hu, and C. Y. Wang, Opt. Lett. **41**, 5142 (2016).

[13]N. Raabe, T. Feng, T. Witting, A. Demircan, C. Brée, and G. Steinmeyer, Phys. Rev. Lett. **119**, 123901 (2017).

[14]C. Manzoni, S. W. Huang, G. Cirmi, P. Farinello, J. Moses, F. X. Kärtner, and G. Cerullo, Opt. Lett. **37**, 1880 (2012).

[15]N. Thire, R. Maksimenka, B. Kiss, C. Ferchud, P. Bizouard, E. Cormier, K. Osvay, and N. Forget, Opt. Express **25**, 1505 (2017).

[16]Z. Chang, Fundamentals of Attosecond Optics (CRC Press, 2011), p. 122.

[17]M. Kakehata, H. Takada, Y. Kobayashi, K. Torizuka, Y. Fujihira, T. Homma, and H. Takahashi, Opt. Lett. **26**, 1436 (2001).

[18]J. A. Armstrong, N. Bloembergen, J. Ducuing, and P. S. Pershan, Phys. Rev. **127**, 1918 (1962).

[19]M. Mehendale, S. A. Mitchell, J. P. Likforman, D. M. Villeneuve, and P. B. Corkum, Opt. Lett. **25**, 1672 (2000).

[20]H. Fattahi, H. G. Barros, M. Gorjan, T. Nubbemeyer, B. Alsaif, C. Y. Teisset, M. Schultze, S. Prinz, M. Haefner, M. Ueffing, A. Alismail, L. Vamos, A. Schwarz, O. Pronin, J. Brons, X. T. Geng, G. Arisholm, M. Ciappina, V. S. Yakovlev, D. E. Kim, A. M. Azzeer, N. Karpowicz, D. Sutter, Z. Major, T. Metzger, and F. Krausz, Optica **1**, 45 (2014).

[21]J. N. Sweetser, D. N. Fittinghoff, and R. Trebino, Opt. Lett. **22**, 519 (1997).

[22]S. Fang, P. Huang, Z. Wei, G. Gao, and K. Zhao, Patent number 201910154175.0 (2018).